Title
Influence of Exit Surface Angle on Drilling Burr Formation

Authors
Min, Sangkee
Dornfeld, David
Nakao, Yohichi

Publication Date
2003

Peer reviewed

Sangkee Min
Post Doctoral Researcher

David A. Dornfeld
Professor, Fellow ASME

Department of Mechanical Engineering,
University of California, Berkeley, CA
94720-1740

Yohichi Nakao
Associate Professor,
Department of Mechanical Engineering,
Kanagawa University,
3-27-1 Rokkakubasi, Kanagawa-ku, Yokohama,
221-8686, Japan

Influence of Exit Surface Angle on Drilling Burr Formation

The influence of an exit surface angle on drilling burr formation was analyzed. The experimental research found that a burr forms on only a certain portion of a hole when an exit surface is not perpendicular to a drill path. An effective interaction angle was newly defined and the concept of degree of plastic deformation was introduced in order to explain this phenomenon. The burr forming location predicted from the effective interaction angle was verified with experimental results. [DOI: 10.1115/1.1596573]

Exit Surface Angle

One of the important parameters affecting burr formation in a drilling process is an exit surface angle. It is defined as the angle between the tangential line to an exit surface and the normal line to a drill path, Fig. 1. In many applications, it can be easily found that an exit surface is neither flat nor perpendicular to the drill path. One of the typical examples is an intersecting hole that is mostly used for lubrication of rotating components. In spite of its wide application, very little research has been conducted on the angled surface workpiece. Stein and Dornfeld [1] conducted experiments on intersecting holes and found that the off-axis offset that induced the variation of the exit angle of intersecting holes was the most dominant factor in burr formation and the burr size is linearly proportional to the exit angle.

The exit surface angle plays an important role in defining the interaction between the cutting edge of the drill and the exit surface. The cutting edge in drilling is traditionally believed to push away the workpiece material so that it acts like a milling cutter similar to oblique cutting at that moment. However, this is only true when the exit surface is normal to the drill path. The burr forms only at a portion of a hole in an angled exit surface while the burr forms along the whole perimeter of a hole in a normal exit surface, Fig. 2. Similar phenomena were observed in intersecting holes, Fig. 3. Kim et al. [2] explained variations in burr sizes in an intersecting hole by an exit angle variation and assumed that the cutting edge always exits from the workpiece. However, the cutting edge may enter into the workpiece depending on feed and speed in the angled exit surface, which in general forms a very small burr or no burr at all. In this study, the interaction between the cutting edge of the drill and the exit surface is discussed in terms of cutting parameters, drill geometries, and workpiece geometries.

Interaction Angle

The term, exit angle, comes from the fact that the cutting edge of the tool exits from the workpiece at an angle derived by the edge and tool geometry. There are mainly two different definitions for the exit angle. The first one is the angle between the line from the center of the tool to the contact point of cutting edge and the tangential line of the exit surface, Fig. 4(a) [3]. But this definition lacks the effect of dynamic motion of the cutting edge with respect to the exit surface. In the direction of movement of the cutting edge, the workpiece may be either cut or pushed away. Hence, the other definition was proposed in order to incorporate this motion. The exit angle is defined as an angle between the cutting velocity vector by rotational speed and the free surface of the workpiece, measured on a plane perpendicular to the surface generated by this cutting edge and parallel to the cutting velocity vector, as shown in Fig. 4(b) [4]. Chern [5] found that the burr size increases as the exit angle increases. However, this definition does not include a feed component in velocity vector and the case when the cutting edge enters into the workpiece.

In general, the feed component of the velocity vector is much smaller than the speed component. Therefore, it does not affect the scalar value of the exit angle much. However, it plays an important role in deciding whether the cutting edge enters or exits when the exit surface is not perpendicular to the drill path. Therefore, it is necessary to define the exit angle more precisely and include the entering motion. The interaction angle is a term expanded from the definition of the abovementioned exit angle. It is defined as a relative angle between the direction of motion of the cutting edge and tangential direction of the workpiece surface in the direction of motion at a moment. The direction of the motion of the cutting edge is the direction of a resultant velocity vector by feed and speed. When the velocity vector of the cutting edge is outside of exit surface line, the interaction angle is positive and vice versa, Fig. 5. It describes both motions of a tool entering and exiting and explains dynamic interaction of the cutting edge onto the workpiece surface.

Kim [2] adopted Kishimoto's [3] definition for the exit angle to explain burr size variation in an intersecting hole. The exit angle in drilling is defined as the angle between the drill axis and the exit surface of the workpiece. The study found that there was a nearly linear relation between the burr size and the exit angle. That is, increasing exit angle produced smaller burrs. This is opposite to the conclusion of Chern's [5] study and Chu's [4] study due to the different use of the exit angle definition. Hence, it is necessary to use a consistent definition of the exit angle in metal cutting.

The interaction angle in drilling can be defined in the same manner as in milling. A drill has two cutting edges: primary cutting edge (lip) and secondary cutting edge (flute edge). The geometrical characteristic of the primary cutting edge is defined by a point angle and that of the secondary cutting edge is defined by a helix angle. However, the interaction angle can be defined in the same way for both cutting edges, Fig. 6.

When the primary cutting edge contacts the exit surface, the velocity vector of the contact point varies depending on its radial distance from the center of the drill. Its radial distance changes as the tip of the drill proceeds in the feed direction. The velocity

Contributed by the Manufacturing Engineering Division for publication in the JOURNAL OF MANUFACTURING SCIENCE AND ENGINEERING. Manuscript received December 2002. Associate Editor: Dong Woo Cho.

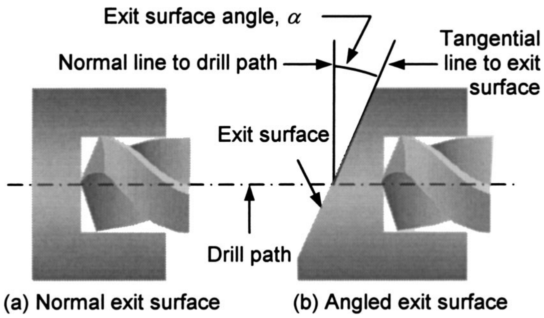

Fig. 1 Definition of an exit surface angle, α

vector for speed is zero at the center and it increases as radial distance from the center increases, Fig. 6(b). This vector always remains on the plane normal to the drill axis. Whereas, the velocity vector for feed is constant and parallel to the drill axis. Hence, the magnitude of the resultant velocity vector at the primary cutting edge increases and its direction becomes close to that of the speed vector as its radial distance increases. In the secondary cutting edge, contact points are at the perimeter of the drill. Hence, all the vectors have the same directions and magnitudes regardless of time.

As the cutting edge emerges from the angled exit surface, the contact point between the cutting edge and the exit surface travels up and down cyclically on the exit surface. Since the velocity vector is always slightly towards the drill path, the cutting edge always exits on a downward exit surface, Figs. 6(c), (e). However, on an upward exit surface, the cutting edge may enter or exit depending on the relative position of the velocity vector and the exit surface vector. In general, if the exit surface angle is larger

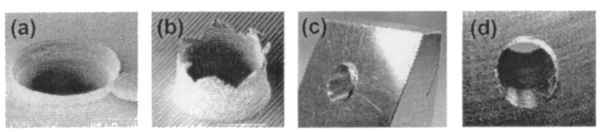

Fig. 2 Difference in burr formation on a normal and an angled exit surface: uniform burr (a) and crown burr (b) of AISI 304L on normal surface and partial burr (c,d) of Aluminum 5052 on angled surface

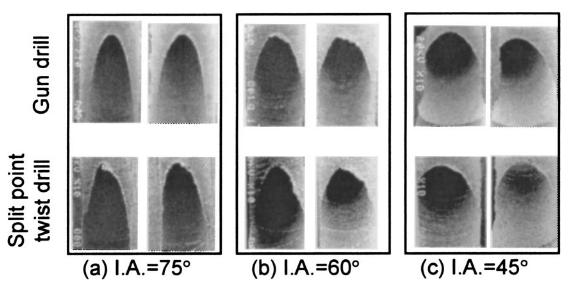

Fig. 3 Burr shapes by different inclination angles and drill [2]

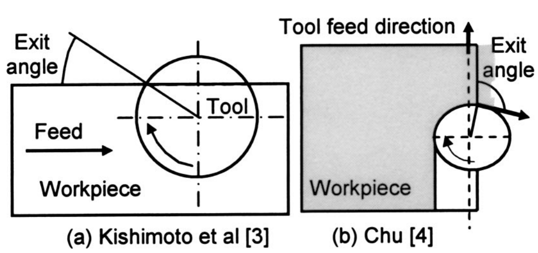

Fig. 4 Definition of the exit angle in milling

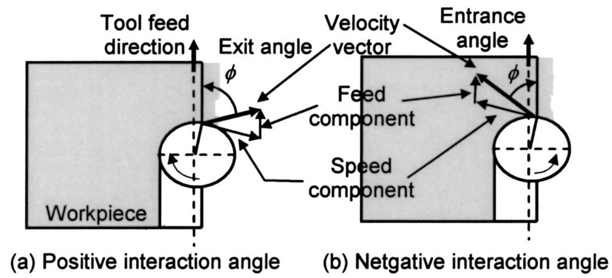

Fig. 5 New definition of the interaction angle in milling

than tangent value of the velocity vector by feed to the velocity vector of speed, then the cutting edge enters, Figs. 6(d), (f). Otherwise, the cutting edge exits even on an upward surface, Fig. 7. From Eq. (1), this can occur if either the exit surface angle, α, is small or the feed is large.

$$\alpha \geqslant \arctan \frac{|\vec{V}_f|}{|\vec{V}_s|} \tag{1}$$

When the drill approaches close to the exit surface, the plastic zone forms in front of the drill. Until it reaches a critical point (a

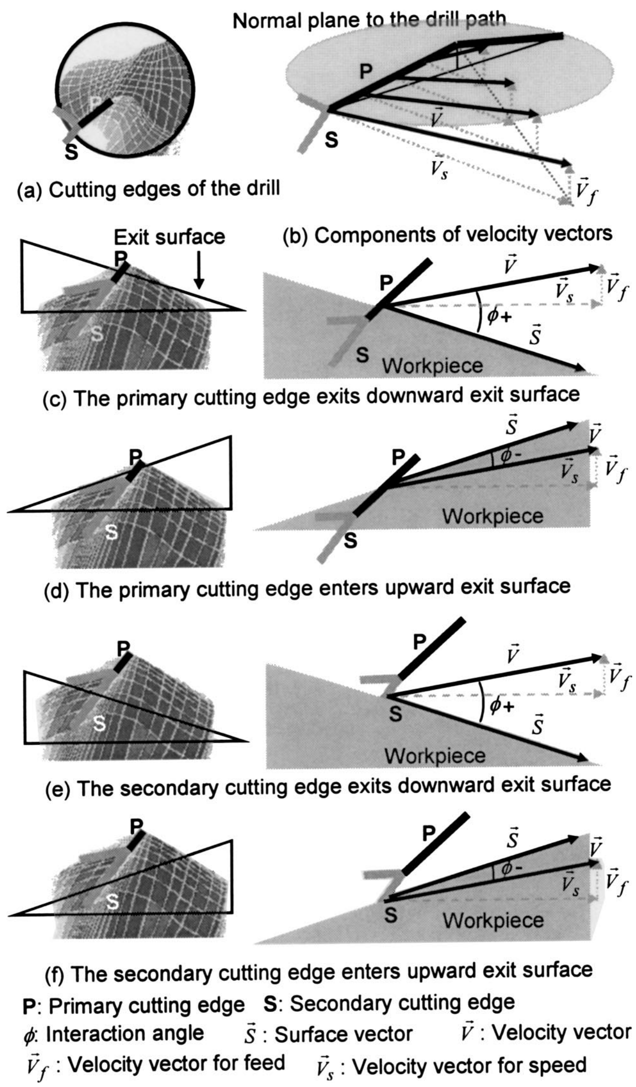

Fig. 6 Definition of the interaction angle in drilling

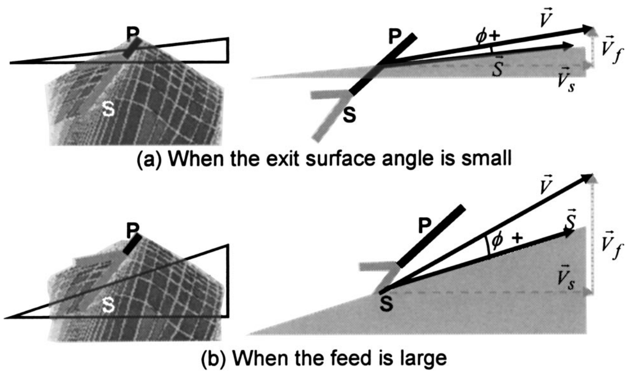

Fig. 7 Interaction angle on upward exit surface

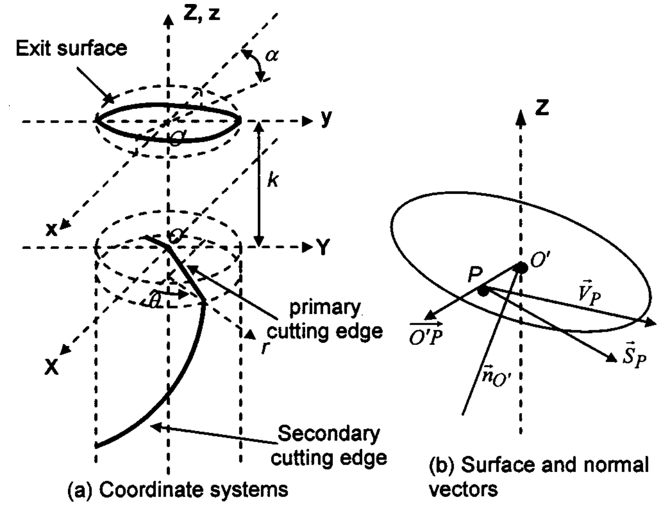

Fig. 9 Coordinate systems and vectors of the point *P* at the primary cutting edge

burr initiation point), cutting is the dominant mechanism [6]. Once the drill reaches the critical point, the exit surface near the center of the drill starts to deform and bending slowly takes over from cutting. Hence, the exit surface topography changes with respect to time. In order to make it simple to define interaction between the cutting edge and the exit surface of the workpiece, the assumption is made that the exit surface remains flat at its original position.

Calculation of the Interaction Angle

The drill is assumed to have a sharp point without chisel edge for simplicity. When the slope of the primary cutting edge, $\bar{p}$, is larger than the exit surface angle, α, the center of the drill reaches the exit surface first, $\bar{p} > \alpha$, Fig. 8.

$$\bar{p} = \frac{1}{2}(\pi - p) \tag{2}$$

The contact time when the center of the drill, O, reaches the exit surface is

$$t_c = \frac{k}{f/60} \tag{3}$$

where f is feed (mm/min) and k is the initial distance between the tip of the drill, O, and the center of the exit surface, O', Fig. 9(a).

After $t = t_c$, the primary cutting edge starts exiting the surface. The angular position of the contact point P is

$$\theta = \theta_0 + 2\pi N t/60 \tag{4}$$

where θ_0 is the initial angular position of the primary cutting edge and N is cutting speed (rpm).

The line from the center of the exit surface, O', to the contact point P is represented as

$$\frac{x}{R\cos\theta} = \frac{y}{R\sin\theta} = \frac{z-k}{R\tan\alpha\cos\theta} \tag{5}$$

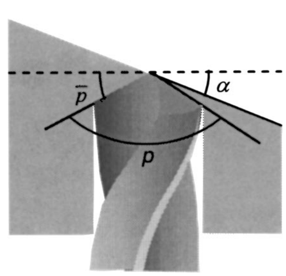

Fig. 8 Small exit surface angle

and the line from the tip of the drill, O, to the contact point P is given as

$$\frac{x}{R\cos\theta} = \frac{y}{R\sin\theta} = \frac{z - ft/60}{-R\tan\bar{p}} \tag{6}$$

where R is the diameter of the drill and α is the exit surface angle.

From Eqs. (5) and (6), the contact point P can be obtained as

$$\begin{aligned} P &= [cR\cos\theta, cR\sin\theta, cR\tan\alpha\cos\theta + k] \\ c &= \frac{ft/60 - k}{R\tan\alpha\cos\theta + R\tan\bar{p}} \end{aligned} \tag{7}$$

The radial distance from the axis of the drill, Z-axis, to the point P is

$$r_P = cR \tag{8}$$

and its velocity vector is expressed as

$$\vec{V}_P = [-2\pi N r_P \sin\theta/60, 2\pi N r_P \cos\theta/60, f/60] \tag{9}$$

The surface vector of the point P in the direction of motion of the primary cutting edge is normal to the directional surface vector, $\vec{n}_{O'}$, and to the line vector, $\overrightarrow{O'P}$, Fig. 9(b).

$$\begin{aligned} &\vec{S}_P \perp \vec{n}_{O'} \perp \overrightarrow{O'P} \\ &\vec{S}_P = [s_{P1}, s_{P2}, s_{P3}] \\ &\overrightarrow{O'P} = [r_P\cos\theta, r_P\sin\theta, r_P\tan\alpha\cos\theta] \\ &\vec{n}_{O'} = [\sin\alpha, 0, -\cos\alpha] \end{aligned} \tag{10}$$

From Eq. (10), the surface vector, $\vec{S}_P$, can be obtained as

$$\begin{aligned} &s_{P1}\sin\alpha - s_{P3}\cos\alpha = 0 \\ &s_{P1}\cos\theta + s_{P2}\sin\theta + s_{P3}\tan\alpha\cos\theta = 0 \\ &\vec{S}_P = \left[\cot\alpha, \frac{2\cot\theta}{\sin 2\alpha}, 1\right] \end{aligned} \tag{11}$$

The interaction angle, ϕ_P, between the velocity vector, $\vec{V}_P$, and the surface vector, $\vec{S}_P$, is

$$\phi_P = \arccos\frac{|\vec{V}_P \cdot \vec{S}_P|}{|\vec{V}_P||\vec{S}_P|} \tag{12}$$

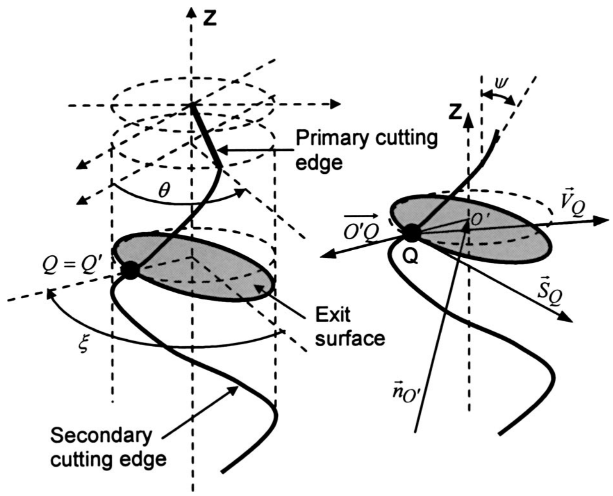

Fig. 10 The surface vector of the point *Q* at the secondary cutting edge

When the secondary cutting edge starts contacting the exit surface as shown in Fig. 10, the radial distance from the axis of the drill, Z-axis, is always R. Hence, the point Q on the secondary cutting edge can be expressed as

$$\vec{S}_Q = \left[\cot\alpha, \frac{2\cot(\theta-\xi)}{\sin 2\alpha}, 1\right] \tag{13}$$

where ξ is an angle to define the point on the secondary cutting edge and ψ is the helix angle of the drill.

The point Q' on the perimeter of the hole on the exit surface is given

$$Q' = [R\cos(\theta-\xi), R\sin(\theta-\xi), k + R\tan\alpha\cos(\theta-\xi)] \tag{14}$$

The two points should be the same point at contact,

$$Q = Q' \tag{15}$$

Hence,

$$k + R\tan\alpha\cos(\theta-\xi) = -R\tan\overline{p} - \frac{R\xi}{\tan\psi} + ft/60 \tag{16}$$

The velocity vector of the point Q, $\vec{V}_Q$, is expressed as

$$\vec{V}_Q = [-2\pi NR\sin(\theta-\xi)/60, 2\pi NR\cos(\theta-\xi)/60, f/60] \tag{17}$$

The surface vector of the point Q in the direction of motion of the secondary cutting edge is normal to the directional surface vector, $\vec{n}_{O'}$, and to the line vector, $\overrightarrow{O'Q}$.

$$\vec{S}_Q \perp \vec{n}_{O'} \perp \overrightarrow{O'Q}$$

$$\vec{S}_Q = [s_{Q1}, s_{Q2}, s_{Q3}] \tag{18}$$

$$\overrightarrow{O'Q} = [R\cos(\theta-\xi), R\sin(\theta-\xi), R\tan\alpha\cos(\theta-\xi)]$$

Then, the surface vector, $\vec{S}_Q$, can be obtained as

$$s_{Q1}\sin\alpha - s_{Q3}\cos\alpha = 0$$

$$s_{Q1}\cos(\theta-\xi) + s_{Q2}\sin(\theta-\xi) + s_{Q3}\tan\alpha\cos(\theta-\xi) = 0 \tag{19}$$

$$Q = \left[R\cos(\theta-\xi), R\sin(\theta-\xi), -R\tan\overline{p} - \frac{R\xi}{\tan\psi} + ft/60\right]$$

Finally, the interaction angle, ϕ_Q between the velocity vector, $\vec{V}_Q$, and the surface vector, $\vec{S}_Q$, is

$$\phi_Q = \arccos\frac{|\vec{V}_Q \cdot \vec{S}_Q|}{|\vec{V}_Q||\vec{S}_Q|} \tag{20}$$

When the slope of the primary cutting edge, $\overline{p}$, is smaller than the exit surface angle, α, the cross point of the primary cutting edge and the secondary cutting edge reaches the exit surface first, $\overline{p} < \alpha$. Then, the same process can be used to calculate the interaction angle.

Prediction of the Interaction Angle

An example of the contact points where the cutting edges meet the exit surface is shown in Fig. 11. The cutting edge comes out near the center of the hole and moves on the thinner portion of the workpiece first. At point 1, the tip of the drill contacts the workpiece surface and proceeds in the positive direction of the Z-axis by feed and rotates in the counter-clockwise direction by speed. From point 1 to point 2, the primary cutting edge cuts the work-

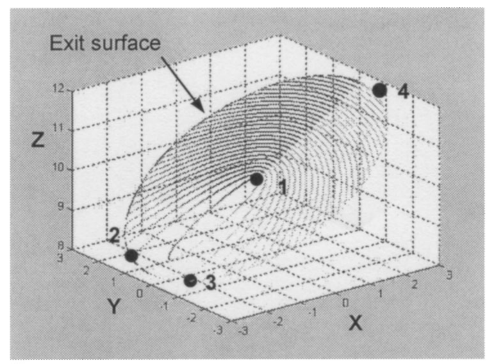

(a) The trajectory of the contact points (black line: tool exits, gray line: tool enters)

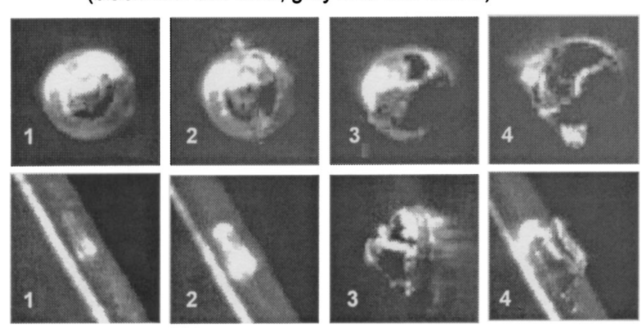

(b) High-speed camera images

Fig. 11 The trajectory of the cutting edges at the 30° angled exit surface

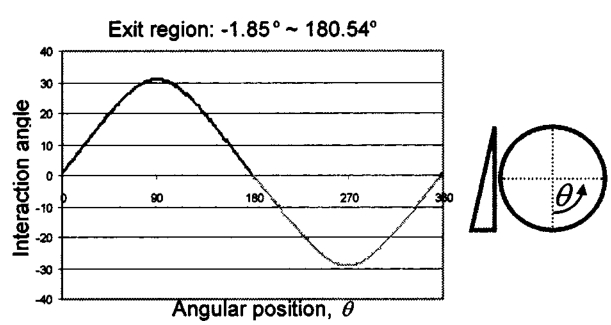

Fig. 12 Variation of the interaction angle at the 30° angled exit surface

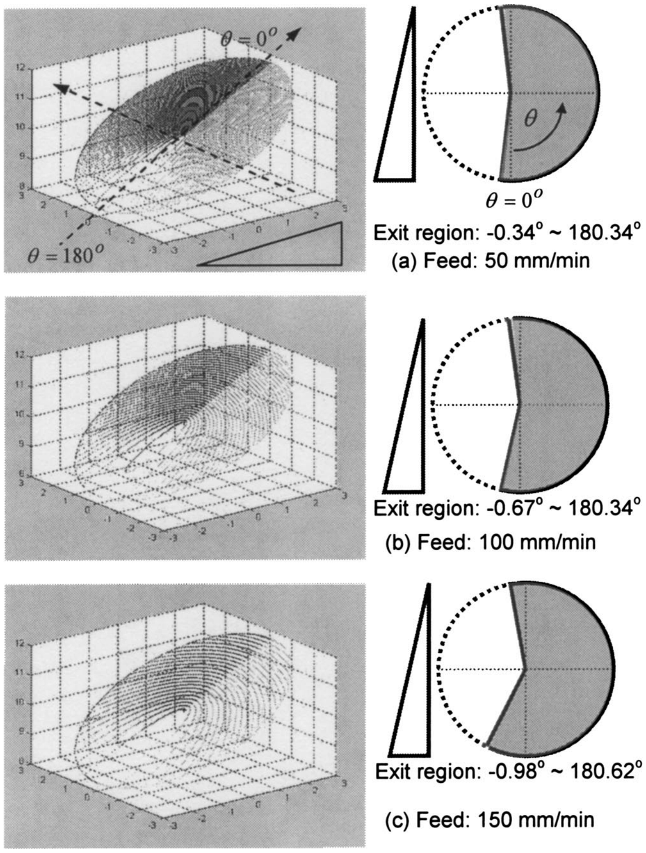

Fig. 13 Influence of feed on the interaction angle (**Speed: 1000 rpm, exit surface angle: 30°**)

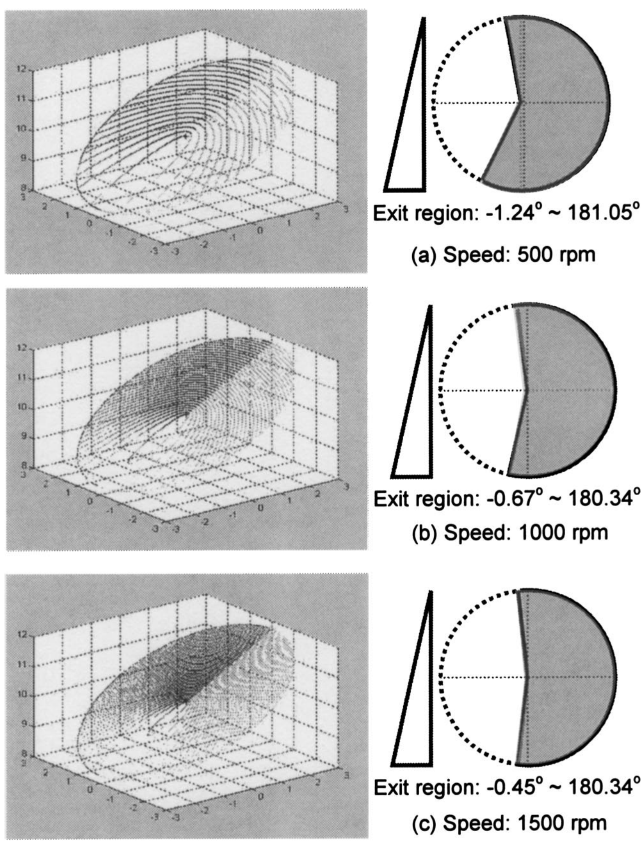

Fig. 14 Influence of speed on the interaction angle (**Feed: 100 mm/min, exit surface angle: 30°**)

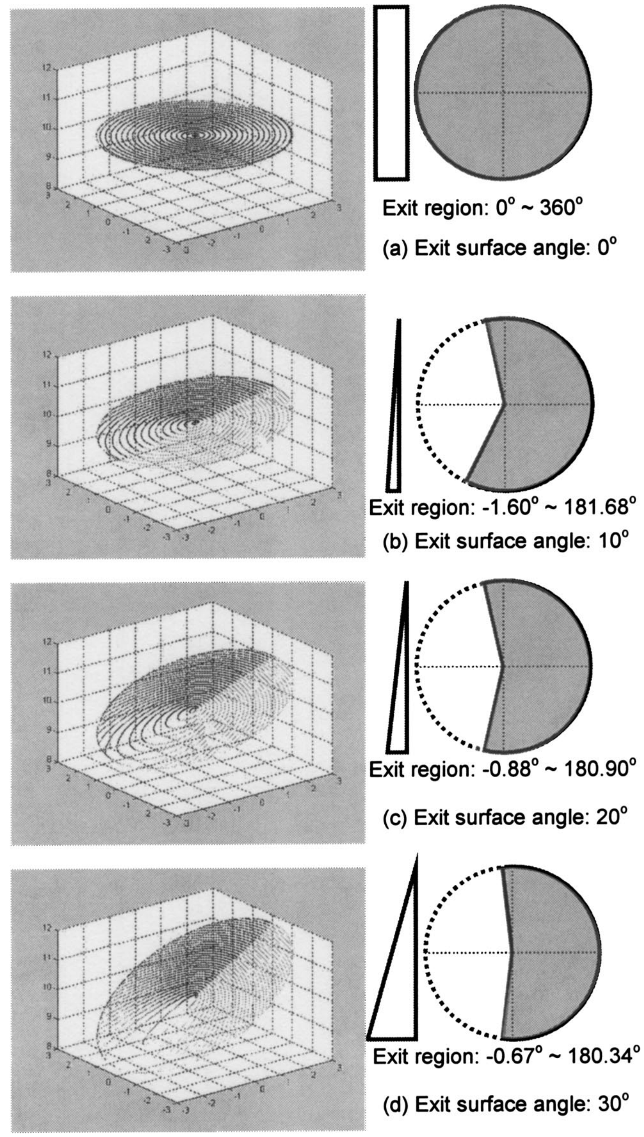

Fig. 15 Influence of the exit surface angle on the interaction angle (**Feed: 100 mm/min, Speed: 1000 rpm**)

piece under the assumption that there is no deformation. From point 2 to point 3, the secondary cutting edge takes over the cutting process and then the primary cutting edge cuts off thicker part of the workpiece again after point 3. This process repeats until point 4. Once the secondary cutting edge reaches point 4, the corner of the cutting edges cuts the workpiece and finishes the hole.

The interaction angle varies along the trajectory. The positive interaction angle means a high probability of burr formation at that point because the cutting edge exits from the workpiece. The negative interaction angle means no burr or low probability of burr formation because the cutting edge enters into the workpiece. In Fig. 11, while the secondary cutting edge moves along the curve from 2 to 3, the interaction angle changes from positive to negative, which means that the secondary cutting edge exits from the workpiece on the black line and enters on the gray line.

Figure 12 shows the interaction angle variation along the perimeter of the hole. The angular position is measured from the positive X-axis in Fig. 11. It shows that the tool exit region is slightly over half of the hole due to the feed component in the velocity vector of the contact point. The feed component slightly lifts up the velocity vector in the Z-axis. Hence, even at the upward exit surface where the surface vector is close to the horizontal surface, the cutting edge exits from the workpiece.

The influence of feed, speed, and the exit surface angle on the interaction angle is investigated. The point angle of the drill is 118°, the helix angle is 30°, and the diameter is 6 mm. The variation of the interaction angle with respect to feed is shown in Fig. 13. As feed increases, the density of trajectories of the contact points decreases while maintaining cutting speed and the exit surface angle constant. The small density of trajectories causes large chip load on the cutting edge and in turn high thrust force. Hence, a larger burr may form at higher feed. The cutting edge exit region is shaded area in the figure. It slightly increases as feed increases, which means a larger burr forming area. The exit region is not symmetric due to the combined effects of feed and the exit surface angle.

The variation of the interaction angle with respect to cutting speed is shown in Fig. 14. As speed increases, the density of trajectories of the contact points increases while maintaining feed and the exit surface angle constant. The cutting edge exit region slightly decreases as cutting speed increases. Hence, a smaller burr forming area appears at higher cutting speed.

The variation of the interaction angle with respect to the exit surface angle is shown in Fig. 15. When the exit surface is perpendicular to the drill path, $\alpha=0°$, the cutting edge always exits from the workpiece. As the exit surface angle increases, the density of trajectories of the contact points increases and its shape becomes more skewed while maintaining feed and cutting speed constant. The cutting edge exit region slightly decreases as the exit surface angle increases. Hence, a smaller burr forming area appears at higher angled exit surface.

Degree of Plastic Deformation

The interaction angle was calculated under the assumption that the topography of the exit surface does not change. However, as the drill approaches close to the exit surface, material in front of the drill experiences plastic deformation. It changes the topography of the exit surface and calculation of the interaction angle requires adjustment accordingly. But it is very difficult to estimate the deformed geometry of the exit surface because the material is not only deformed but also cut. Therefore, the stiffness of material keeps changing as the drill advances, which makes the estimation of the exit surface geometry challenging.

Park [7] investigated the influence of the exit surface angle using his finite element model. He found that burr formation decreases as the exit surface angle increases. The pivoting point that initiates plastic bending leading a large burr formation appears very close to the machined surface when the exit surface angle is 30°. As the exit surface angle decreases, the pivoting point moves farther from the machined workpiece and causes a larger burr.

The same theory can be applied to the cross-sectional diagram of drilling on an angled exit surface at any moment. In the bottom part of the workpiece where the exit surface angle is 30° in Fig. 16, the pivoting point appears very close to the machined surface, which results in no burr or a very small burr. As the exit surface angle decreases, the pivoting point moves farther from the machined surface. This can be explained by the stiffness of the workpiece material. As the cutting edge approaches the exit surface, material is being cut until the pivoting point appears at the exit surface. Once the pivoting point appears, transition from cutting to bending occurs. When the exit surface angle is large, the bottom part of the workpiece is stiffer than that of smaller exit surface angle. Hence, thicker a workpiece sustains the thrust force and delays formation of the pivoting point and thus transition to bending.

The upper part of the workpiece in Fig. 16 contains thinner material that enables early formation of the pivoting point far from the machined surface and early transition to bending from cutting. In fact, the exit surface angle of the upper part of the workpiece can be seen as a negative angle. Then, it is consistent to Park's results.

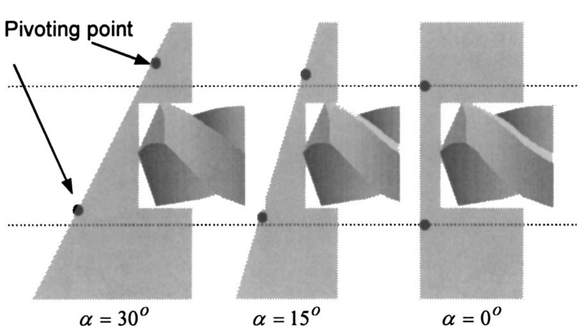

Fig. 16 Variation of the pivoting point

Likely Burr Forming Area

Even though the degree of plastic deformation theory does not give a quantitative measure in predicting the exact burr location, a likely location of burr formation can be estimated. The exit surface angle varies depending on the location of contact point P. Hence, the effective surface angle, $\bar{\alpha}$, is defined as the angle between the line vector, $\overrightarrow{O'P}$, and the tangent vector, $\vec{t}$, which lies on the normal plane to the drill path, Fig. 17.

The line vector, $\overrightarrow{O'P}$, and the tangent vector, $\vec{t}$, are

$$\begin{aligned}\overrightarrow{O'P}&=[\cos\theta,\sin\theta,\tan\alpha\cos\theta]\\ \vec{t}&=[\cos\theta,\sin\theta,0]\end{aligned} \tag{21}$$

Then, the effective exit surface angle, $\bar{\alpha}$, is given as

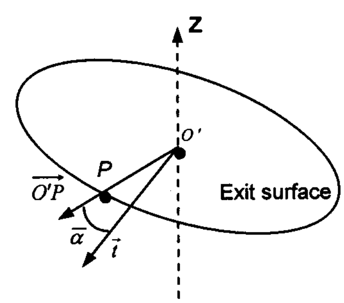

Fig. 17 Definition of the effective exit surface angle

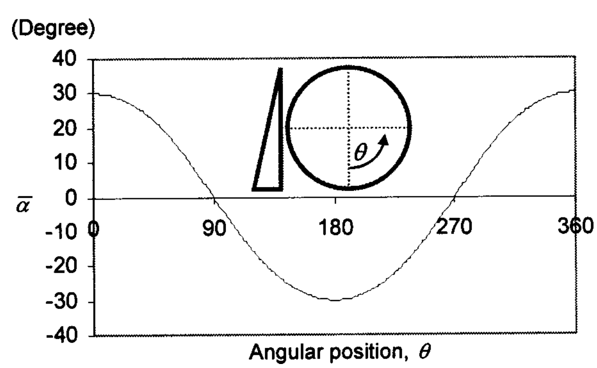

Fig. 18 Variation of the effective exit surface angle at the 30° angled exit surface

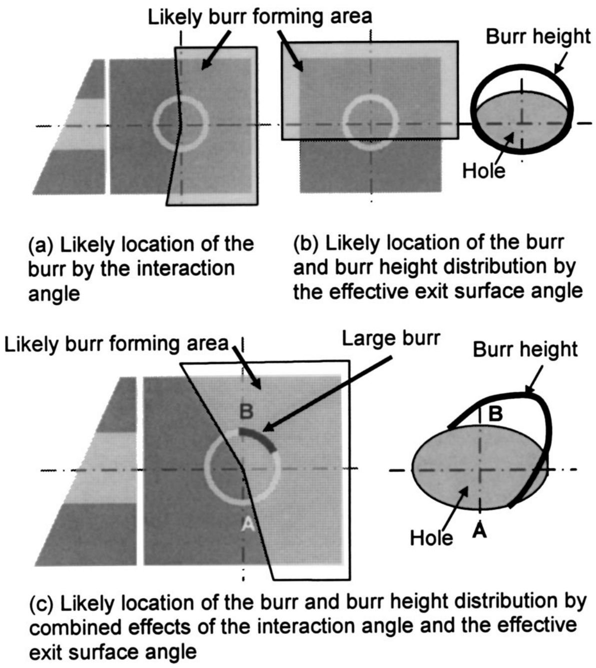

Fig. 19 Likely burr forming area

$$\overline{\alpha}=\arccos\frac{|\overrightarrow{O'P}\cdot\vec{t}|}{|\overrightarrow{O'P}||\vec{t}|} \tag{22}$$

The variation of the effective exit surface angle when the exit surface angle is 30° is shown in Fig. 18. The effective exit surface angle is 30° at the center of the bottom part of the workpiece and decreases as the angular coordinate increases. When it is negative, the exit surface lies beneath the normal plane of the drill path. Hence, a large burr may form. The burr size is inversely proportional to the effective exit surface angle [7]. Hence, either the smallest burr or no burr may form at $\theta=0°$ where the workpiece has the thickest exit surface and the highest stiffness. The largest burr may form at $\theta=180°$ where the workpiece has the thinnest exit surface and the lowest stiffness without considering the interaction angle effects.

The interaction angle defines where the burr may form but the deformation of the exit surface is not considered. Therefore, the likely burr forming area is almost the entire right half of the hole with a slight shift by feed and the exit surface angle, Fig. 19(a). The effective exit surface angle describes the degree of plastic deformation and, thus, burr size distribution, Fig. 19(b). By combining these two factors, the likely burr forming area can be represented as in Fig. 19(c). Due to high stiffness at the bottom, A, a burr does not form even though the cutting edge exits. Therefore, the start point of a burr forming area is shifted in the counter-clockwise direction. Near the top, B, the interaction angle is negative. However, due to the large plastic deformation of the thin material near B, the real value of the interaction angle becomes positive. Therefore, the cutting edge is still exiting and the end point of a burr forming area is shifted in the counter-clockwise direction.

The experimental results are shown in Fig. 20. In the experiments, the burr forming area increases as feed increases except when the feed is 120 mm/min. This matches the prediction from the interaction angle calculation. However, as mentioned earlier, due to the effective exit surface angle, overall area is shifted in the counter-clockwise direction. Hence, considering both the interaction angle and the effective exit surface angle, the likely burr forming area matches well with the experimental results.

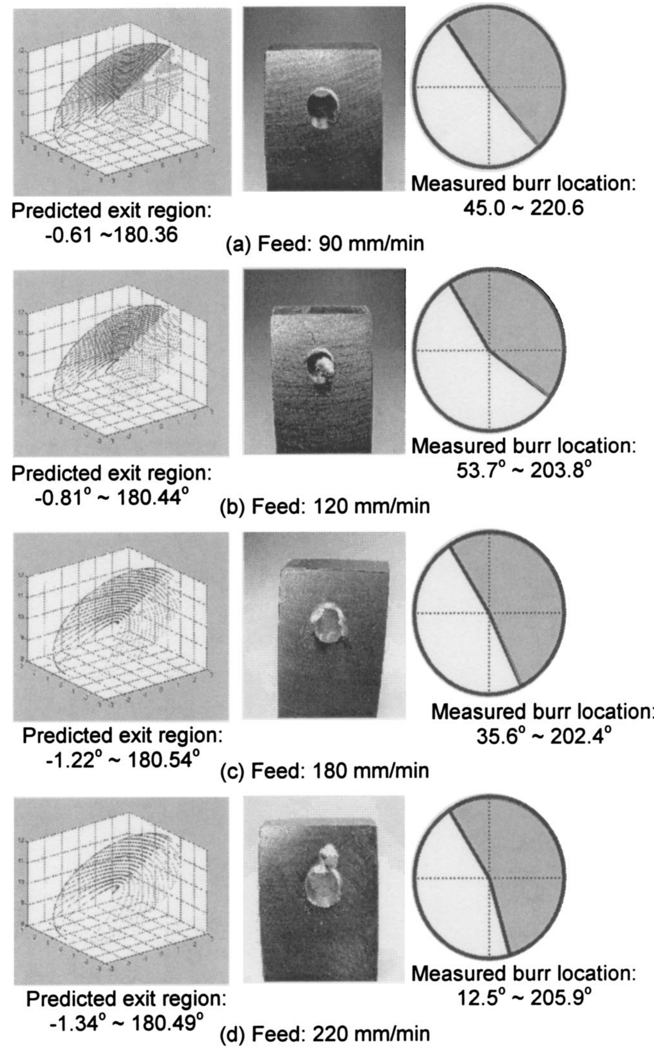

Fig. 20 Burr location measurements (Speed: 1000 rpm, Exit surface angle: 30° Drill: straight shank twist drill with 6 mm diameter, 118° point angle, 32° helix angle, workpiece: Aluminum 5052)

Conclusions

An interaction angle that defines the interaction between the cutting edge and the exit surface was proposed under the assumption that the exit surface geometry does not change. It includes dynamic motion of the cutting edge induced by feed and speed. When the interaction angle is positive, the cutting edge exits from the workpiece and vice versa. It can predict the likely burr forming area that can be represented as the positive interaction angle. The likely burr forming area increases as feed increases, speed decreases, and the exit surface angle decreases.

An effective exit surface angle was proposed in order to incorporate the change of the exit surface geometry during drilling. Due to the plastic deformation at the end of cutting process, the exit surface geometry changes. Depending on the angular position of the exit surface, the effective exit surface angle changes. A small negative exit surface angle promotes early initiation of the bending mechanism and results in a large burr. Hence, thinner parts of the workpiece may have a larger burr.

The interaction angle dictates exiting and entering of the cutting edge. Hence, it predicts the likely burr forming area. The effective exit surface angle defines the size of burr and shifts the likely burr forming area computed by the interaction angle in the rotational direction of the drill. The experimental results show good agreements with the prediction.

Acknowledgments

This work is supported by the Consortium on Deburring and Edge Finishing (CODEF) at the University of California, Berkeley (http://lma.Berkeley.edu/codef).

Nomenclature

P = primary cutting edge
S = secondary cutting edge
N = cutting speed (rpm)
O = tip of the drill
O' = center of the exit surface
P = contact point of the primary cutting edge
Q = contact point of the secondary cutting edge
R = drill diameter (mm)
$\underline{p}$ = point angle of the drill
p = slope of the primary cutting edge
f = feed (mm/min)
k = initial distance between O and O'
t_c = initial contact time
α = exit surface angle
ϕ = interaction angle
θ = angular position
θ_0 = initial angular position of the primary cutting edge
ξ = angular position of the secondary cutting edge
ψ = helix angle of the drill
$\vec{S}$ = surface vector
$\vec{S}_p$ = surface vector of the point P
$\vec{S}_Q$ = surface vector of the point Q
$\vec{V}$ = velocity vector
$\vec{V}_f$ = velocity vector for feed
$\vec{V}_s$ = velocity vector for speed
$\vec{V}_p$ = velocity vector of the point P
$\vec{V}_Q$ = velocity vector of the point Q
$\vec{n}$ = normal vector of the point O'
$\vec{t}$ = normal vector of the point O'

References

[1] Stein, J. M., and Dornfeld, D. A., 1996, ''Influence of Workpiece Exit Angle on Burr Formation in Drilling Intersecting Holes,'' Transactions of NAMRI/SME, **24**, pp. 39–43.
[2] Kim, J., Dornfeld, D. A., and Furness, R., 1999, ''Experimental Study of Burr Formation in Drilling of Intersecting Holes With Gun Drill and Twist Drills,'' Technical Papers of NAMRI/SME, pp. 39–44.
[3] Kishimoto, W., Miyake, T., Yamamoto, A., Yamanaka, K., and Takano, K., 1981, ''Study of Burr Formation in Face Milling,'' Japanese Society of Precision Engineering, **15**(1), pp. 51–52.
[4] Chu, C. H., 2000, ''Integrated Edge Precision Machining,'' Ph.D. dissertation, Dept. of Mech. Eng., University of California at Berkeley.
[5] Chern, G. L., 1993, ''Analysis of Burr Formation and Breakout in Metal Cutting,'' Ph.D. dissertation, Dept. of Mech. Eng., University of California at Berkeley.
[6] Min, S., Dornfeld, D. A., Kim, J., and Shyu, B., 2001, ''Finite Element Modeling of Burr Formation in Metal Cutting,'' International Journal of Machining Science and Technology, **5**(3), pp. 307–322.
[7] Park, I. W., 1996, ''Modeling of Burr Formation Processes in Metal Cutting,'' Ph.D. dissertation, Dept. of Mech. Eng., University of California at Berkeley.